Figure S1

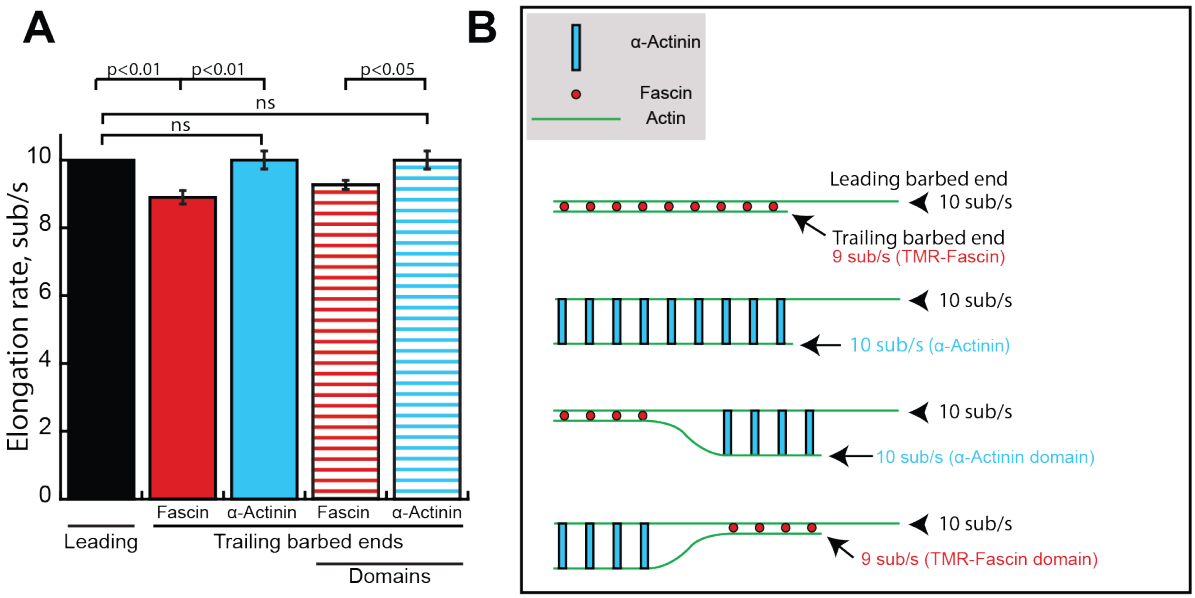
A
p<0.01
p<0.01
p<0.05
ns
ns
Elongation rate, sub/s
10
8
6
4
2
0
Fascin
α-Actinin
Fascin
α-Actinin
Leading
Trailing barbed ends
Domains
B
α-Actinin
Fascin
Actin
Leading barbed end
10 sub/s
Trailing barbed end
9 sub/s (TMR-Fascin)
10 sub/s
10 sub/s (α-Actinin)
10 sub/s
10 sub/s (α-Actinin domain)
10 sub/s
9 sub/s (TMR-Fascin domain)

Figure S1. Measurement of elongation rates of actin filament leading and trailing barbed ends in parallel two-filament bundles, related to Figure 3.
(A) Graph of the leading (black bar) and trailing barbed end elongation rates. Solid red and cyan bars are elongation rates from trailing ends from reactions containing only one type of bundler, fascin (red) or α-actinin (cyan). Striped bars represent the elongation rates of trailing ends from reactions containing both fascin and α-actinin mixed together at concentrations where domains form. Striped bars represents trailing ends within a fascin domain (red striped) or α-actinin domain (cyan striped), n corresponds to a single actin bundle, n>8, error bars represent the SEM.
(B) Cartoon depicting two-filament bundle types and associated elongation rates depicted in (A). Trailing barbed ends bundled by fascin grow at 90% of non-bundled actin barbed ends, while there is no detectable difference in the elongation rates of α-actinin-bundled trailing ends from non-bundled ends.

Figure S2

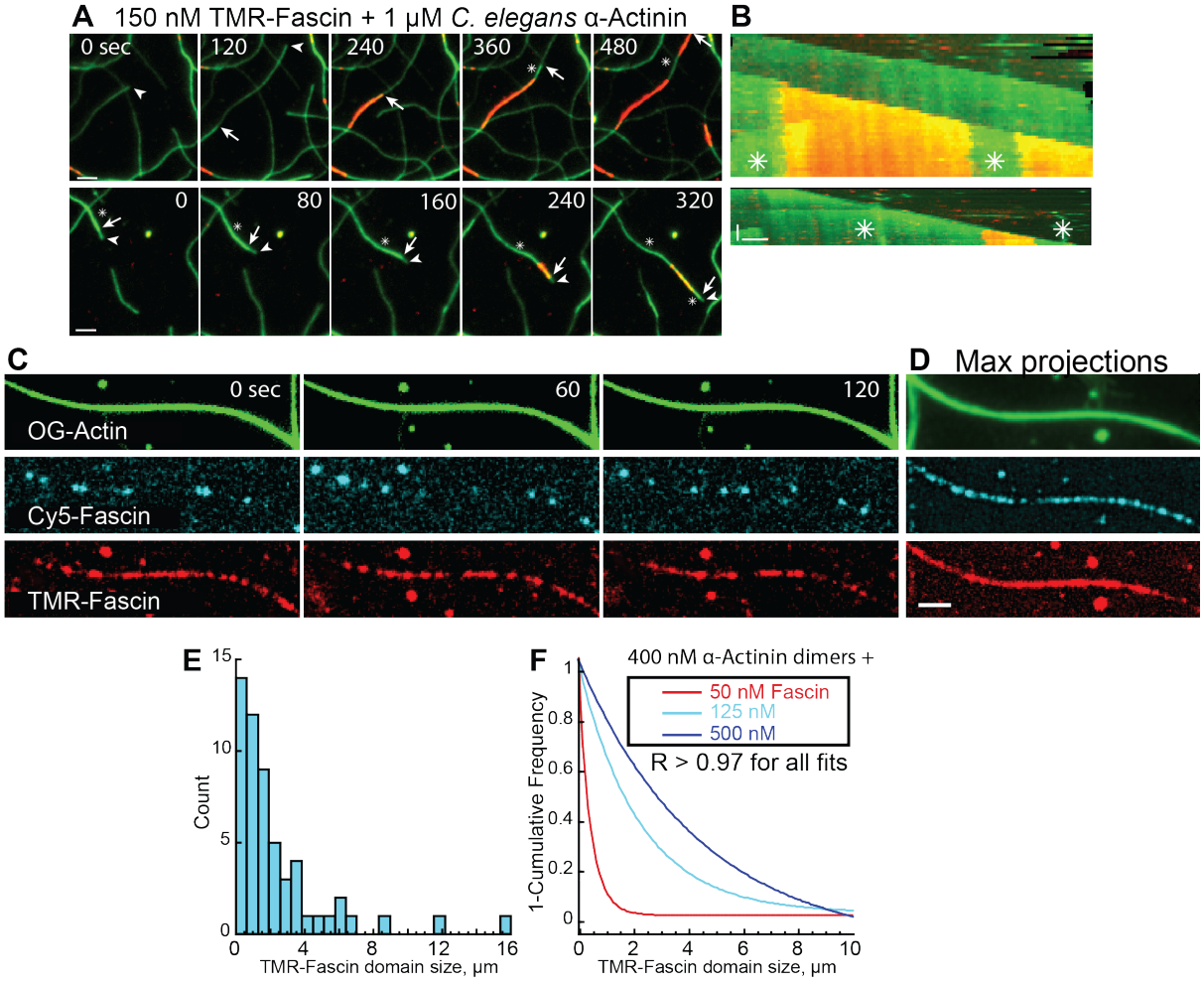
A 150 nM TMR-Fascin + 1 μM C. elegans α-Actinin
0 sec
120
240
360
480
0
80
160
240
320
B
C
0 sec
60
120
OG-Actin
Cy5-Fascin
TMR-Fascin
D Max projections
E
Count
TMR-Fascin domain size, μm
F
400 nM α-Actinin dimers +
50 nM Fascin
125 nM
500 nM
R > 0.97 for all fits
1-Cumulative Frequency
TMR-Fascin domain size, μm

Figure S2. TMR-fascin forms domains when mixed with α-actinin, related to Figure 3.
(A and B) Multi-color TIRFM of 1.5 μM actin (15% Oregon green-actin), 100 nM TMR-fascin and 400 nM *C. elegans* α-actinin dimers.
(A) Merged time-lapse micrographs (scale bar=2 μm), and (B) corresponding kymographs of filament length (x-axis scale bar=2 μm) over time (y-axis scale bar=200 sec) for two representative bundles. Arrowheads and arrows indicate leading and trailing barbed ends of two-filament bundles. Asterisks indicate bundled regions devoid of TMR-fascin.
(C and D) Three-color TIRFM assay containing 1.5 μM actin (15% Oregon-green labeled), 2.0 nM Cy5-fascin (cyan) and 50 nM TMR-fascin (red).
(C) Montage taken from a representative TIRFM time-lapse movie.
(D) Maximum projection of 60 frames (t =0 to 180). Scale bar=2 μm.
(E and F) Length distributions of TMR-fascin domains formed in the presence of α-actinin.
(E) Histogram of the lengths of TMR-fascin domains formed in the presence of 125 nM TMR-fascin and 400 nM α-actinin dimers.
(F) 1-cumulative frequency of TMR-fascin domain lengths in reactions with 400 nM α-actinin dimers and 50, 125 or 500 nM TMR-fascin. Data fit to a single exponential decay function, the average length τ plotted in Figure 3H, was derived from the single exponential decay curve fits.

Figure S3

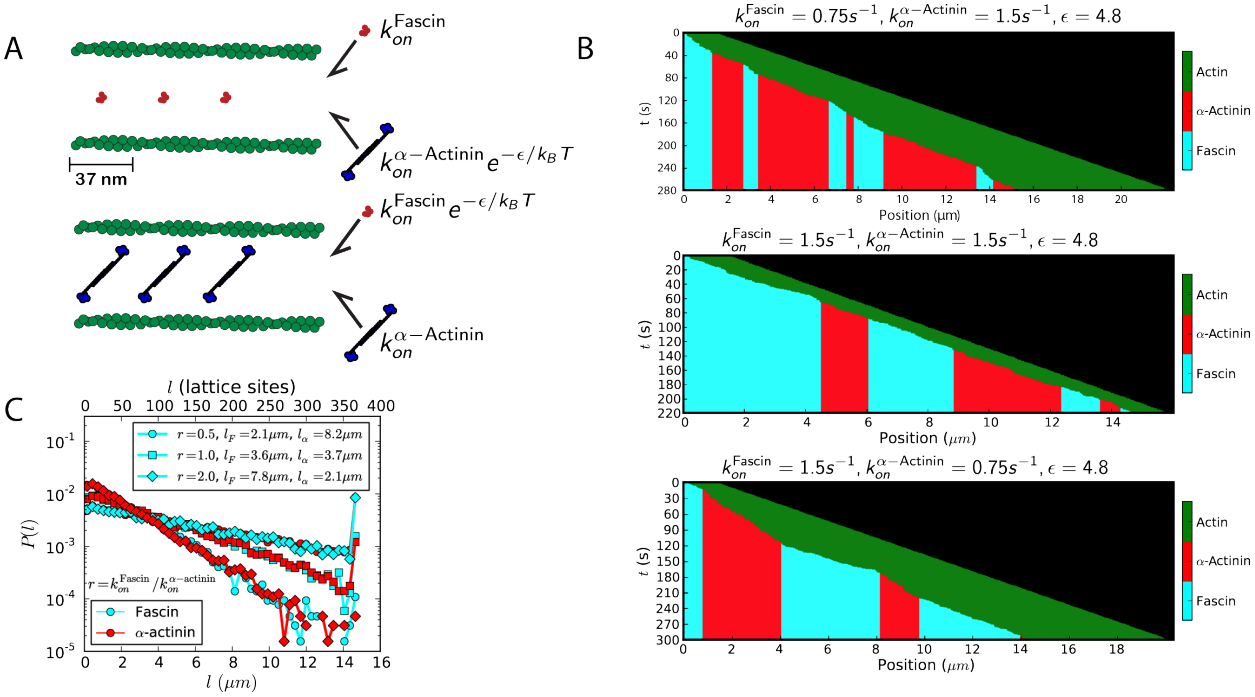
A
k_{on}^{Fascin}
$k_{on}^{\alpha-\text{Actinin}} e^{-\epsilon/k_B T}$
37 nm
$k_{on}^{\text{Fascin}} e^{-\epsilon/k_B T}$
$k_{on}^{\alpha-\text{Actinin}}$
B
$k_{on}^{\text{Fascin}} = 0.75s^{-1}$, $k_{on}^{\alpha-\text{Actinin}} = 1.5s^{-1}$, $\epsilon = 4.8$
t (s)
Position (μm)
Actin
α-Actinin
Fascin
$k_{on}^{\text{Fascin}} = 1.5s^{-1}$, $k_{on}^{\alpha-\text{Actinin}} = 1.5s^{-1}$, $\epsilon = 4.8$
t (s)
Position (μm)
Actin
α-Actinin
Fascin
$k_{on}^{\text{Fascin}} = 1.5s^{-1}$, $k_{on}^{\alpha-\text{Actinin}} = 0.75s^{-1}$, $\epsilon = 4.8$
t (s)
Position (μm)
Actin
α-Actinin
Fascin
C
l (lattice sites)
$r=0.5$, $l_F=2.1\mu m$, $l_\alpha=8.2\mu m$
$r=1.0$, $l_F=3.6\mu m$, $l_\alpha=3.7\mu m$
$r=2.0$, $l_F=7.8\mu m$, $l_\alpha=2.1\mu m$
$r = k_{on}^{\text{Fascin}} / k_{on}^{\alpha-\text{actinin}}$
Fascin
α-actinin
P(l)
l (μm)

Figure S3. Computational model of fascin and α-actinin segregation, related to Figure 3.
(A) Cartoon illustrating the computational model. A lattice represents binding sites on a preformed and extending crosslinked bundle. Adding of new crosslinkers is slowed down if the type of the crosslinker is different from the one preceding it.
(B) Example kymographs for 3 sets of parameters. Because the two crosslinkers studied have approximately the same affinity for a bundle, the ratio of on rates is approximately the ratio of concentrations. Hence show are ratios r=0.5, r=1, and r=2. A preformed actin filament growing at 20 subunits/sec (~53 nm/sec) is shown only for illustrative purposes and is not part of the model.
(C) Probabilities of seeing domains of crosslinkers fascin (cyan) and α-actinin of a given length in μm (bottom axis) and lattice sites (top axis). Data is shown for the three sets of parameters given in (B), with average domain lengths from exponential fits for fascin and α-actinin given in the inset. Fascin domain lengths extracted in this manner for a wider range of parameters appear in the main Figure 3H.

Figure S4

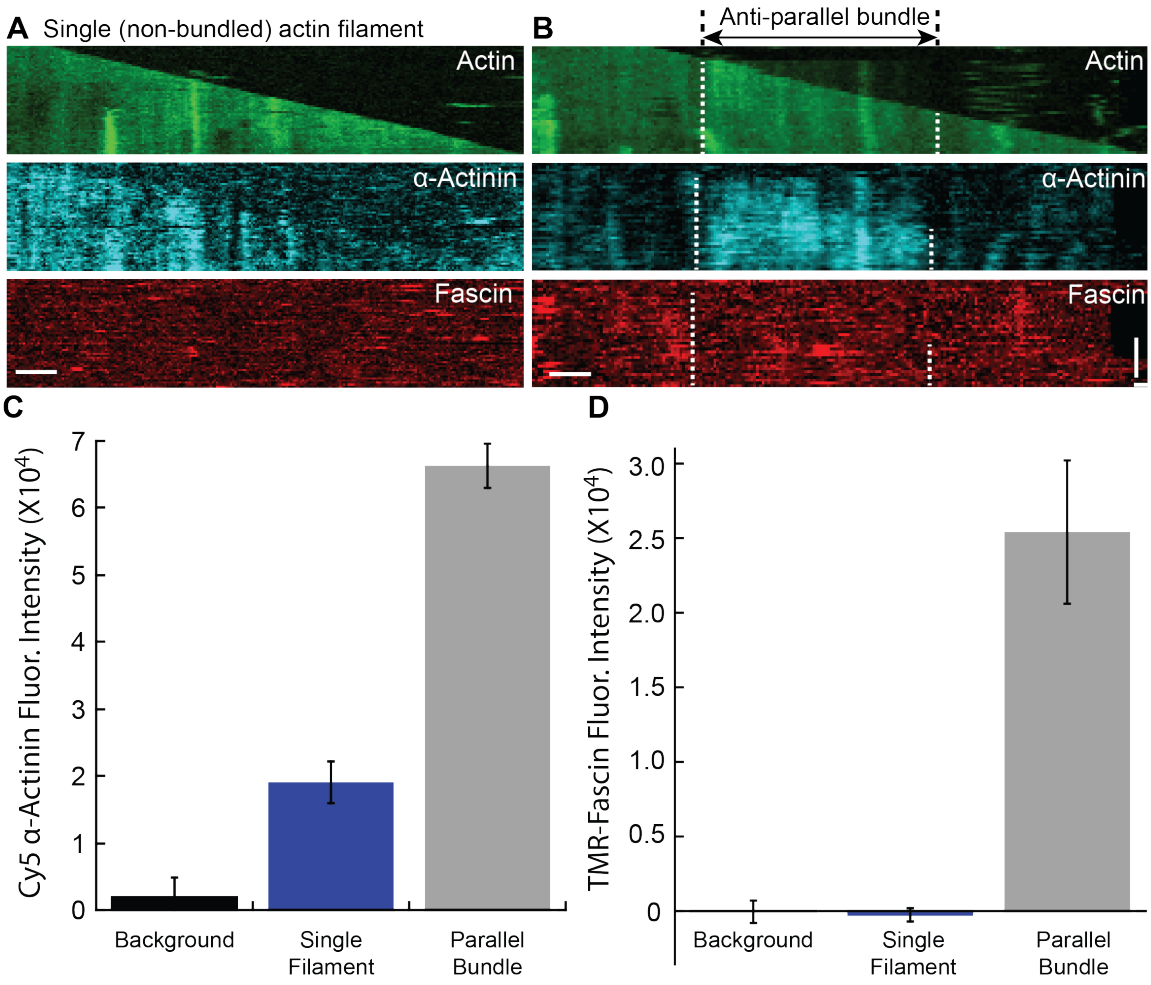
A Single (non-bundled) actin filament
B
Anti-parallel bundle
Actin
α-Actinin
Fascin
Actin
α-Actinin
Fascin
C
Cy5 α-Actinin Fluor. Intensity (X10^4)
0
1
2
3
4
5
6
7
Background
Single Filament
Parallel Bundle
D
TMR-Fascin Fluor. Intensity (X10^4)
0
0.5
1.0
1.5
2.0
2.5
3.0
Background
Single Filament
Parallel Bundle

Figure S4. α-Actinin binds to single filaments and anti-parallel bundles, whereas fascin does not, related to Figure 3.
Three-color TIRFM of 1.5 μM actin (15% Oregon green-actin), 400 nM Cy5-α-actinin dimers (cyan) and 100 nM TMR-fascin (red).
(A) Kymographs of a single non-bundled filament.
(B) Kymographs of an anti-parallel two-filament bundle denoted by dotted lines.
(C and D) Quantification of (C) α-actinin and (D) fascin fluorescence on single and anti-parallel bundled filaments. n >5 (actin bundles), error bars represent SEM.

Figure S5

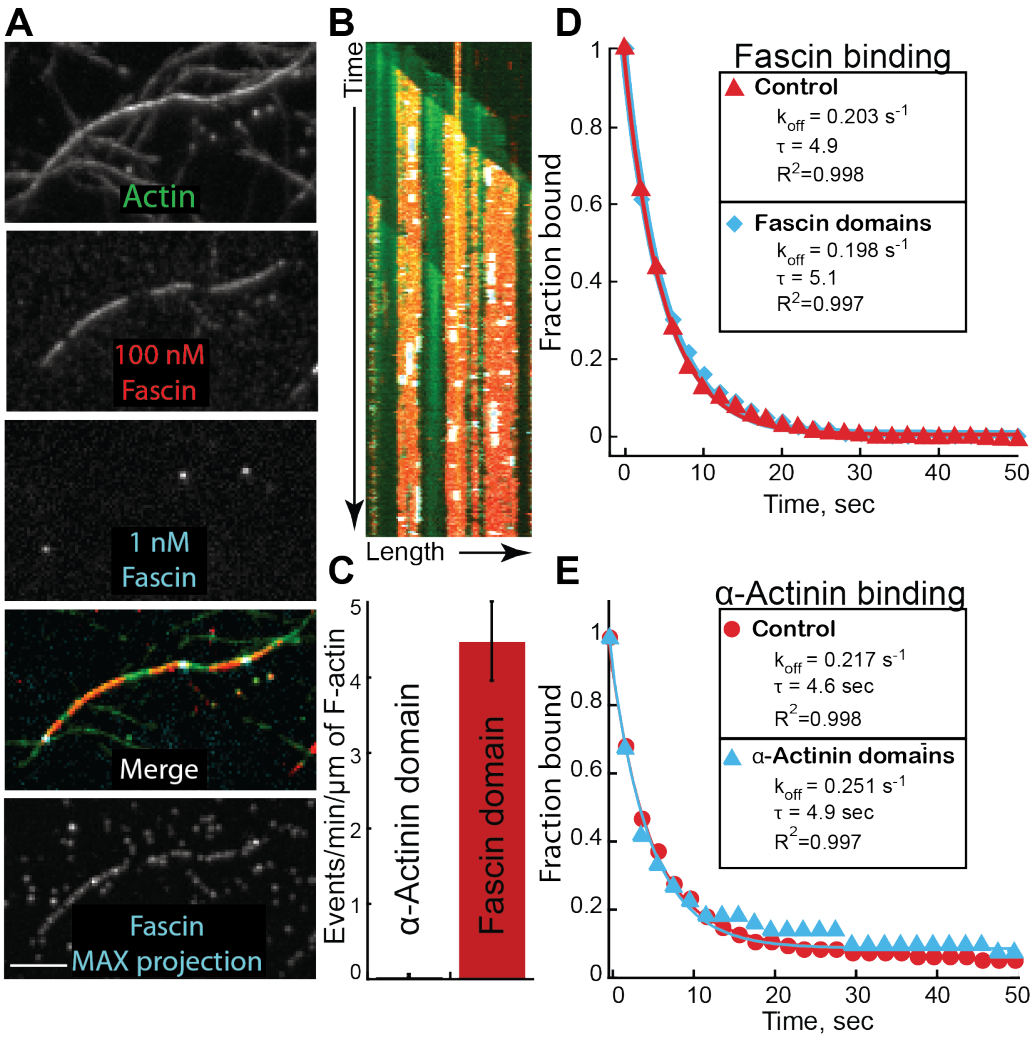
A
Actin
100 nM
Fascin
1 nM
Fascin
Merge
Fascin
MAX projection
B
Time
Length
C
Events/min/µm of F-actin
α-Actinin domain
Fascin domain
D
Fascin binding
Control
k_{off} = 0.203 s^{-1}
τ = 4.9
R^2=0.998
Fascin domains
k_{off} = 0.198 s^{-1}
τ = 5.1
R^2=0.997
Fraction bound
Time, sec
E
α-Actinin binding
Control
k_{off} = 0.217 s^{-1}
τ = 4.6 sec
R^2=0.998
α-Actinin domains
k_{off} = 0.251 s^{-1}
τ = 4.9 sec
R^2=0.997
Fraction bound
Time, sec

Figure S5. Fascin and α-actinin are dynamic molecules with similar residence times on two-filament bundles, related to Figure 3.
(A) Fluorescent micrographs from three-color TIRFM of 1.5 μM actin (15% Oregon green-actin), 1 nM Cy5-fascin, 100 nM TMR-fascin and 400 nM α-actinin dimers.
(B) Corresponding kymograph of filament length (x-axis scale bar=2 μm) over time (y-axis scale bar=100 sec).
(C) Quantification of the number of detectable Cy5-fascin single molecule binding events (over 500 sec) observed on either two-filament parallel α-actinin domains or TMR-fascin domains, represents a single fascin or α-actinin domain, n > 7, error bars represent SEM.
(D) Single exponential fits of the fraction of single Cy5-fascin molecules bound on TMR-fascin domains in the absence (red curve) or presence of α-actinin (blue curve).
(E) Single exponential fits of the fraction of single TMR-α-actinin molecules bound to α-actinin domains in the absence (red curve) or presence of Cy5-fascin (blue curve).

Figure S6

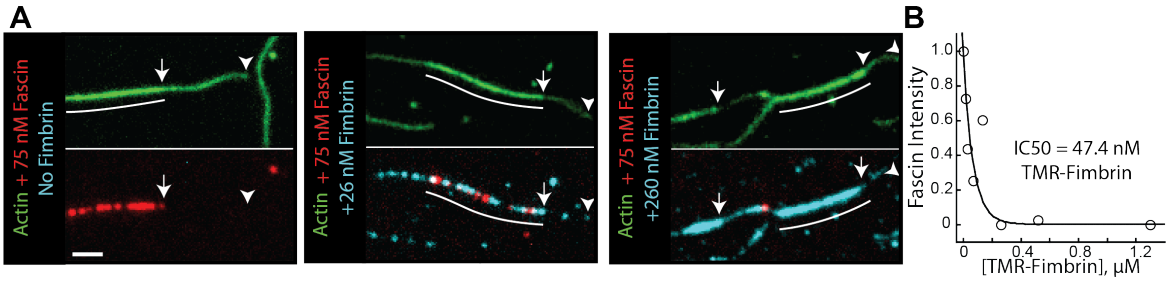
A
Actin + 75 nM Fascin
No Fimbrin
Actin + 75 nM Fascin
+26 nM Fimbrin
Actin + 75 nM Fascin
+260 nM Fimbrin
B
Fascin Intensity
1.0
0.8
0.6
0.4
0.2
0
IC50 = 47.4 nM
TMR-Fimbrin
0
0.4
0.8
1.2
[TMR-Fimbrin], µM

Figure S6. Fimbrin and fascin compete on two-filament parallel bundles, related to Figure 5.
(A) Micrographs of three-color TIRFM of 1.5 μM actin (15% Oregon green-actin, top), 75 nM Cy5-fascin (cyan, bottom), and either in the absence (left) or presence of 26 nM (middle) or 260 nM (right) TMR-fimbrin (red, bottom). White line indicates parallel two-filament bundles. Arrows and arrowheads indicate trailing and leading barbed ends. Scale bars=2 μm.
(B) Dependence of Cy5-fascin intensity associated with two-filament bundles on the concentration of TMR-fimbrin.

Supplemental Experimental Procedures

Plasmid construction:
Constructs were prepared by standard restriction digest and ligation or infusion (Clontech) following PCR amplification (iProof; Bio-Rad). *C. elegans* α-actinin isoform B, was amplified from *C. elegans* cDNA and put into pet21a expression vector at the BamHI/NotI sites, where a C-terminal His tag was added. 6X His-tagged human α-actinin4, was cloned into Pet21a E. coli expression vector at the EcoRI/XhoI. GST-Hsfascin construct has been previously described [S1] as well as SpFim1 [S2] 6XHis-SNAP-espins 2A and 3B were cloned into a ProEX HTA *E. coli* expression vector.

Protein purification:
Fission yeast fimbrin SpFim1 was purified as described [S2]. Both Human α-actinin4 and *C. elegans* α-actinin and SNAP-espin E2B were expressed in *E. coli* BL21-Codon Plus(DE3)-RP (Stratagene) cells induced by 0.5 mM isopropyl β-D-thiogalactopyranoside (IPTG, Sigma-Aldrich) for 16 hours at 16°C. Bacterial pellets were collected by centrifugation and resuspended in extraction buffer (50 mM NaH_2PO_4, pH 8.0, 500 mM NaCl, 10% glycerol, 10 mM imidazole, 10 mM betamercaptoethanol [βME]) with phenylmethylsulfonyl fluoride (PMSF) and protease inhibitors. Resuspended pellets were homogenized by passing through an Emulsiflex-C3 (Avestin, Ottawa, ON, Canada). Clear lysate was obtained by removing cell debris from the homogenate by centrifugation at 30,000g and 50,000g consecutively. Purified proteins were isolated by incubating the lysate with Talon Metal Affinity Resin (Clontech, Mountain View, CA). Bound recombinant proteins were eluted in Talon elution buffer (50 mM NaH_2PO_4, pH 8.0, 500 mM NaCl, 10% glycerol, 250 mM imidazole, 10 mM βME) and dialyzed overnight into Source Q buffer (20 mM Tris-HCl, pH 8.5, 50 mM NaCl, 5% glycerol, 0.01% NaN_3, 1 mM DTT). Dialyzed proteins were further clarified by a 5.0 mL Source Q column (GE Healthcare Life Science), eluted with a linear gradient from 300 to 700 mM NaCl. Pure α-actinin was dialyzed into α-actinin storage buffer (20 mM tris-HCl, pH 7.9, 100 mM NaCl, 0.2 mM EDTA, 0.01% NaN_3, 1 mM DTT, and 10% glycerol). Actin was purified from rabbit skeletal muscle acetone powder (Pel-Freez) by a cycle of polymerization and depolymerization, and gel filtration [S3]. Gel-filtered actin was labeled with Oregon green iodoacetimide on Cysteine 374 [S4]. Mouse capping protein and human fascin were expressed in *E. coli* and purified as described [S1, S5].

Protein labeling:
SpFim1 was labeled as previously described [S6]. Human fascin and both Human and *C. elegans* α-actinin were labeled with either Cy5-Monomaleimide (GE Healthcare) or TMR-6-Maleimide (Life Technologies, Grand Island, NY). The dyes were resuspended in DMF to a concentration of 10 mM (TMR) or 1 mM (Cy5). Purified proteins were first dialyzed overnight into labeling buffer (20 mM Tris-HCl, pH 7.9, 100 mM NaCl, 0.2 mM EDTA, 0.01% NaN_3, and 10% glycerol) to remove DTT. A 3 to 5 Molar excess of dye was added to the reaction and allowed to label at 4°C overnight. The labeling reaction was quenched and the dye removed by 3 serial dialyses in 500 mL of fascin storage buffer (labeling buffer + 1 mM DTT) for 2 hours each. Proteins containing the SNAP fusion were labeled with SNAP-surface-549 or SNAP-surface-647 (New England BioLabs) according to manufacturer's protocols except that proteins were incubated with the dye overnight at 4°C.

Actin filament sedimentation assay:
Conditions: 10 mM imidazole, pH 7.0, 50 mM KCl, 1 mM $MgCl_2$, 1 mM EGTA, 0.5 mM DTT, 0.2 mM ATP, 90 μM $CaCl_2$. Actin filaments preassembled for 45 min at 25°C from 15 μM Mg-ATP actin monomers. Assembled actin was then incubated with a range of concentrations of accessory protein(s) for 20 minutes at 25˚C, and then spun at 10,000g (low-speed) for 20

minutes at 25˚C. In α-actinin-fascin competition assays, α-actinin was added first, and incubated for 20 min, and then fascin was added and incubated for an additional 20 minutes. Equal volumes of supernatant and pellet were separated by 12.5% SDS-polyacrylamide gel electrophoresis, stained with Coomassie Blue for 20 minutes, and destained for 16 hours. Gels were analyzed by densitometry on an Odyssey Infrared Imager (LI-COR Biosciences, Lincoln, NE).

TIRFM assay:
Conditions: 10 mM imidazole pH 7.0, 50 mM KCl, 1 mM $MgCl_2$, 1 mM EGTA, 0.5 mM DTT, 0.2 mM ATP, 50 μM $CaCl_2$, 15 mM glucose, 20 μg/mL catalase, 100 μg/mL glucose oxidase, and 0.5% methylcellulose (400 cP) at 25°C. Actin final concentration was always 1.5 μM where 10–33% was Oregon green-labeled. Images were from 0.5-20 seconds on an IX-71 microscope (Olympus) fit with through-the-objective TIRF illumination and an iXon EMCCD camera (Andor Technology, South Windsor, CT). For two- and three-color TIRFM, we cyclically imaged Oregon-green actin (one frame, 488-nm excitation for 50 ms) and SNAP-549 or TMR (one frame, 561-nm excitation for 50 ms) and Cy5 or SNAP-647 (one frame, 638-nm excitation for 50 ms).

Flow channel preparation:
Microscope slides and coverslips (#1.5; Fisher Scientific) were washed for 30 min with acetone and for 10 min with 95% ethanol, were sonicated for 2 h with 2% Hellmanex III detergent (Hellma Analytics), incubated for 1-2 h with piranha solution (66.6% H_2SO_4, 33.3% H_2O_2), washed thoroughly with deionized water, then with 95% ethanol and incubated for 18 h with 1 mg/mL mPeg-Silane (5,000 MW) in 95% ethanol, pH 2.0. Exposure to air was minimized. Coverslips and slides were stored at 4°C in parafilmed petri dishes and used within 1-2 weeks. Parallel strips of double-sided tape were placed on the coverslip to create multiple flow chambers on a single piece of passivated glass.

Bead motility assay:
Two micron diameter carboxylate polystyrene microspheres (2.6% solids-latex suspension; Polysciences, Eppelheim, Germany) were coated with GST-pWA as followed [S7]. GST-pWA–coated beads were mixed with a motility medium containing 4 μM actin monomers (1% Oregon green-actin), 4 μM human profilin 1, 100 nM Arp2/3 complex, 20 nM Capping Protein with and without 50 nM TMR-labeled-α-actinin and Cy5-labeled-fascin, in TIRF polymerization buffer (10 mM Imidazole (pH 7.0), 50 mM KCl, 1 mM $MgCl_2$, 1 mM EGTA, 50 mM DTT, 0.2 mM ATP, 50 mM $CaCl_2$, 15 mM glucose, 20 mg/mL catalase, 100 mg/mL glucose oxidase, and 0.5% (wt/vol) methylcellulose 400 centipoise). Motile beads were imaged after 15 minutes of polymerization on an inverted microscope (Ti-E; Nikon, Melville, NY) with a confocal scan head (CSU-X; Yokogawa Electric, Musashino, Tokyo, Japan), 491, 561, and 642 nm laser lines (Spectral Applied Research, Richmond Hill, Ontario, Canada) and imaged with a HQ2 charge-coupled device camera (Roper Scientific, Trenton, NJ). METAMORPH software (Molecular Devices, Eugene, OR) was used to control the microscope. Z-stacks were acquired using a 100x oil-immersion objective every 1 μm. Images were reconstructed and analyzed using the software ImageJ (NIH, Bethesda, Maryland, USA, http://imagej.nih.gov/ij/, 1997-2014). Fluorescence ratios were determined using the central, single plane of motile beads. Background-subtracted fluorescence values were measured for each fluorescent protein in the comet tail region and in the protrusion region. The fluorescence ratios (Figure 2E and 2F) were determined by dividing fascin fluorescence by actin fluorescence. The ratio for fascin/α-actinin fluorescence was determined similarly.

Interfilament distance measurement by TIRFM:
To generate two-filament bundles where each filament was a different color, 5 μM of Mg-ATP-actin was initially assembled for 45 min at room temperature. These filaments were then incubated with an equimolar amount of Alexa-647-phalloidin, diluted in TIRF buffer and flowed into the chamber. We then initiated the assembly of 1.5 μM actin, 33% OG-labeled, with TMR-fascin and α-actinin and gently flowed this mixture into the chamber. A fraction of the bundles contained one Alexa-647-filament and one OG-actin filament. If the two-filament bundle had TMR-signal we scored it as a fascin bundle, whereas if no TMR-signal was present we scored it as an α-actinin bundle.

The distance between actin filaments within both fascin and α-actinin bundles is expected to be less than the pixel size (< 100 nm) in our images. To calculate this sub-pixel value we analyzed the data similar to a previously described method [S8]. Briefly, we first corrected for any differences between channels due to the optics of our setup by imaging 100 nm TetraSpeckTM microspheres (Life Technologies) to find the centroids of the diffraction-limited spots (~20/field) in both our OG-actin and 647-Phalloidin channels. The centroids of the spots in each channel were aligned in imageJ using a rigid body transformation. Fluorescence intensity within the two-filament was due to either Oregon-green on one filament or Alexa-647 on the other. We constructed a line that was snapped to the brightest pixel along the Oregon-green actin filament. The coordinates of this line were fit with a polynomial equation that was differentiated to construct a line that was normal to the actin filament at that position. The intensity for both the OG-actin and Alexa-647-phalloidin across the normal line was profiled at each pixel along the filament. The intensities for all of the line scans in a single region were averaged, resulting in two distributions, (OG-actin and alexa-647-phalloidin) which could be fit with a Gaussian function. The centers of the Gaussian were found and the separation between the two profiles was calculated. This procedure was repeated across multiple two-filament bundles (α-actinin and fascin) in different experiments to yield an average interfilament distance.

Negative staining electron microscopy:
For EM visualization, 1.5 μM actin monomers were polymerized with 250-500 nM α-actinin, 1-2 μM fascin, or both bundling proteins in 1xKMEI (50 mM KCl, 1 mM $MgCl_2$, 1 mM EGTA, and 10 mM Imidazole pH 7.0) for 30 minutes. This solution was then applied to Formvar and carbon-coated 400 mesh copper grids for 1 min, washed with 1xKMEI, and negatively stained with 1% (w/v) uranyl acetate for 1 min, blotted, and dried. Visualization of the bundles using transmission electron microscopy was performed by on a FEI Tecnai G2 Spirit microscope at 120kV. Images were captured on a Gatan CCD camera. Bundle parameters were measured using ImageJ.

Cooperative kinetic model
As mentioned in the main text and as can be seen in movies S1 and S2, the moving front of a bundle appears to move unidirectionally. Neither major regression of the front nor exchange of crosslinker types within a bundle are observed at the temporal and spatial resolution of the experiments. Hence, we choose to model the extension of the bundle as a simple kinetic process on a lattice of binding sites where only the next open site can be modified. For the data in Fig 3H, we created a lattice of 400 virtual binding sites, corresponding to two actin filaments coming together of length ~15 μm (400 binding sites separated by 37nm) This length was chosen because it corresponds to a reasonable length of a bundle to be observed in vitro, but was long enough to remove edge effects occurring in experiments where large bundles cannot be observed due to only part of the growing bundle being observed in the view of the microscope.

In the simulations, there are two types of crosslinkers that can occupy a site, A and B. We associate with each a rate of addition to a bundle of like-type, k_{on}^{A} and k_{on}^{B}. In the particular case of this paper, because the affinity for a bundle of like type is approximately equivalent for the

two crosslinkers studied, these rates can be thought of as directly proportional to concentration. We assume a simple model of cooperativity where both types of crosslinkers add an energetic penalty for the other crosslinker to add, and take that penalty to be the same for both crosslinkers. Hence in the case where a crosslinker of type A occupies a site, the rate of addition for crosslinker B is changed to $k_{on}^{B}e^{-\epsilon/k_BT}$, where $k_B$is Boltzmann's constant and T is temperature. Similarly, occupancy of site B means the addition rate of A will be changed to $k_{on}^{A}e^{-\epsilon/k_BT}$.

To initiate the simulation, the first two sites contain A with probability $k_{on}^{A}/(k_{on}^{A}+k_{on}^{B})$ and B with probability $k_{on}^{B}/(k_{on}^{A}+k_{on}^{B})$. This corresponds to the hypothesis that starting a bundle of type A or B is approximately proportional to concentration. We then perform a standard kinetic monte carlo procedure to fill in the rest of the remaining sites. We fix k_{on}^{A} arbitrarily which only sets the unimportant unit of "time", which leaves only two tuning parameters, k_{on}^{B}/k_{on}^{A}, and ϵ. For each pair of these two parameters tested we run 5000 independent simulations. From these runs we compute the average repeat length of A's and B's. Choosing ε=4.8 kBT gave the best fit to the data in Figure 3H.

Supplemental References

S1. Vignjevic, D., Yarar, D., Welch, M. D., Peloquin, J., Svitkina, T., and Borisy, G. G. (2003). Formation of filopodia-like bundles in vitro from a dendritic network. J Cell Biol *160*, 951–962.

S2. Skau, C. T., and Kovar, D. R. (2010). Fimbrin and tropomyosin competition regulates endocytosis and cytokinesis kinetics in fission yeast. Curr. Biol *20*, 1415–1422.

S3. Spudich, J. A., and Watt, S. (1971). The Regulation of Rabbit Skeletal Muscle Contraction I. Biochemical studies of the interaction of the tropomyosin-troponin complex with actin and the proteolytic fragments of myosin. J. Biol. Chem. *246*, 4866–4871.

S4. Kuhn, J. R., and Pollard, T. D. (2005). Real-Time Measurements of Actin Filament Polymerization by Total Internal Reflection Fluorescence Microscopy. Biophysical Journal *88*, 1387–1402.

S5. Palmgren, S., Ojala, P. J., Wear, M. A., Cooper, J. A., and Lappalainen, P. (2001). Interactions with PIP2, ADP-actin monomers, and capping protein regulate the activity and localization of yeast twinfilin. J Cell Biol *155*, 251–260.

S6. Skau, C. T., Courson, D. S., Bestul, A. J., Winkelman, J. D., Rock, R. S., Sirotkin, V., and Kovar, D. R. (2011). Actin Filament Bundling by Fimbrin Is Important for Endocytosis, Cytokinesis, and Polarization in Fission Yeast. J. Biol. Chem. *286*, 26964–26977.

S7. Reymann, A.-C., Suarez, C., Guérin, C., Martiel, J.-L., Staiger, C. J., Blanchoin, L., and Boujemaa-Paterski, R. (2011). Turnover of Branched Actin Filament Networks by Stochastic Fragmentation with ADF/Cofilin. Mol. Biol. Cell *22*, 2541–2550.

S8. James, J. R., and Vale, R. D. (2012). Biophysical mechanism of T-cell receptor triggering in a reconstituted system. Nature *487*, 64–69.